

Investigation for Contact Interface of Mechanical Lap Joint Fabricated with High-Temperature Superconducting Conductor Using X-Ray Microtomography^{*)}

Weixi CHEN, Satoshi ITO, Noritaka YUSA and Hidetoshi HASHIZUME

Graduate School of Engineering, Tohoku University, Sendai, Miyagi 980-8579, Japan

(Received 29 November 2019 / Accepted 21 February 2020)

Joint winding of high-temperature superconducting (HTS) helical coil with conductor segments that are connected using bridge-type mechanical lap joints is considered as a promising method of fabricating magnet for a FFHR heliotron-type fusion reactor. Although methods for joining large-scale HTS conductor has been developed using the “simple-stack” and “joint-piece” procedures, the difference between these procedures is unclear. In this study, the two-row-four-layer joint samples were fabricated via the two joining procedures and compared in terms of contact resistivity. Joint thickness and joint resistance were measured; the contact area at the contact interface was evaluated using an X-ray computer tomography scan, to obtain the precise contact resistivity of the joint. The contact resistivity of the sample fabricated via the “simple-stack procedure” ranged from 2.41 - 5.15 p Ω m², whereas that of the sample fabricated using the “joint-piece procedure” ranged from 1.98 - 6.07 p Ω m². There was no significant difference between the procedures in terms of contact resistivity range. Considering the characteristics of joint thickness and location distribution of each lap joint, the inhomogeneous joining pressure was the primary factor affecting contact resistivity. As the similarity of electrical performances of the two procedures was clarified, future studies should focus on the manufacturability of large-scale joints.

© 2020 The Japan Society of Plasma Science and Nuclear Fusion Research

Keywords: high-temperature superconducting magnet, joint-winding, mechanical lap joint, contact resistivity, X-ray computer tomography scan

DOI: 10.1585/pfr.15.2405014

1. Introduction

Joint-winding high-temperature superconducting (HTS) helical coil [1–3] has been proposed as a promising alternative to magnet for the large helical device (LHD)-type fusion reactor FFHR series [4, 5]. The coil is wound by half- or single-pitch stacked tapes assembled in rigid structure (STARS) conductor segments, which consist of simply-stacked rare-earth barium copper oxide (REBCO) tapes embedded in copper and stainless-steel jackets. A bridge-type mechanical lap joint is utilized for joining these segments. The joining portions of the segments have REBCO tape stacks arranged in a staircase structure, and these portions are joined using a joint piece, such that the staircase structure for face-to-face contacts lies between the two REBCO tapes. The conductor segments and the area of the joint piece pressed together with an indium foil inserted in between them. A previous study examined a bridge-type mechanical lap joint of STARS conductors involving three rows and fourteen layers of 10-mm-wide REBCO tape, and achieved 118 kA energized at 4.2 K and 0.45 T [6]. The joint resistance was 1.8 n Ω which corresponds to a joint resistivity (i.e., product of the joint resistance and nominal joint area) of 10 p Ω m² at 4.2 K;

this value is sufficiently low from the perspective of cooling power. However, the joint resistivity corresponds to a joint resistivity of 30 p Ω m² at 77 K, which accounts for the temperature dependence of joint resistivity, and this value was larger than that of a single-tape lap joint [7].

Recently, we developed a low-temperature heat treatment method involving temperature below the melting point of indium; this treatment reduces the joint resistance and its variations in single-tape lap joints [8–10]. This technique was also applied to improve the joint resistance of a large-scale conductor joint. A bridge-type mechanical lap joint that contained one row and thirteen layers of 10-mm-wide REBCO tape was fabricated using an unintegrated joint piece (“simple-stack procedure”) and heat treated at 90°C; it exhibited joint resistivities in the range of 5.0 - 12.5 p Ω m² at 77 K [11]. Another joint of the STARS conductor consisting of two rows and four layers of 12-mm-wide REBCO tape was fabricated using an integrated joint piece (“joint-piece procedure”) and heat treated at 120°C; it had a joint resistivity of 4.2 - 7.1 p Ω m² at 77 K, and 2.1 - 3.6 p Ω m² at 4.2 K [12]. Although these studies have reported improvements in joint performance, the factors that led to improvements in the two previously mentioned procedures have not been determined, owing to the difference in the heating temperature and geometry of

author's e-mail: wchen@karma.qse.tohoku.ac.jp

^{*)} This article is based on the presentation at the 28th International Toki Conference on Plasma and Fusion Research (ITC28).

the REBCO tapes. As electrical joint performance is one of the important factors for evaluating the performance of a coil, it is essential to clarify this difference and improve the procedure of joint fabrication.

To analyze the joint performance, it is necessary to understand the conditions inside the conductor. X-ray computer tomography (CT) scan is known for its excellent non-destructive inner inspection ability, which can be utilized to analyze the filament conditions of superconducting materials [13, 14], and to trace the superconducting strands in the cable-in-conduit conductor (CICC) [15]. We have previously employed this technique for observing and evaluating the contact area of a single-tape lap joint [7, 16]; this method can also be used for quantitative evaluation of the contact area of a multiple-tape lap joint.

In this study, bridge-type mechanical lap joints were fabricated using a “simple-stack procedure” and a “joint-piece procedure,” under identical joining conditions and for identical REBCO tape arrangements. The electrical resistance of the contact interface (contact resistance) was estimated based on the current-voltage characteristics at 77 K. An X-ray CT scan was utilized to quantitatively analyze the contact area and precisely evaluate the contact resistivity (i.e., product of the contact resistance and the contact area). The obtained contact resistivity was applied to analyze the difference between the two fabrication procedures.

2. Material and Method

2.1 Sample preparation

To fabricate the joint samples, 12-mm-wide copper-stabilized REBCO tapes (SCS12050-AP, SuperPower Inc, Schenectady, NY, USA, I_c : 466 A at 77 K and self-field) were used. The thicknesses of the layers constituting the tapes from top to bottom is as follows: copper (20 μm), silver (2 μm), REBCO (1 μm), buffer layers (less than 0.2 μm), Hastelloy substrate (50 μm), silver (2 μm), and copper (20 μm). Due to the difference in the interlayer resistance arising due to the manufacturing process [17], random sections of the REBCO tapes were tested to measure the interlayer resistance (resistance of the interfaces of REBCO/silver and silver/copper), using a contact-probing current transfer length (CTL) method [18]. Furthermore, 50- μm -thick and 100- μm -thick indium foils were prepared to fabricate the joint sample.

A two-row-four-layer joint geometry was chosen for the samples. Figure 1 depicts a schematic of the joint. The joint contains eight layers of bridge-type joints, in which each layer has two single lap joints. Here, the steps at the joint were denoted as A–H, and the rows were denoted as M and N. Each lap joint is denoted $J_{i,j}$. The subscripts i and j represent the individual layer number ($i = 1 - 8$) and joint number ($j = 1$ in the left and $j = 2$ in the right), respectively. The length of each single lap joint was 10 mm, and the length of the 100- μm -thick indium foil set on the

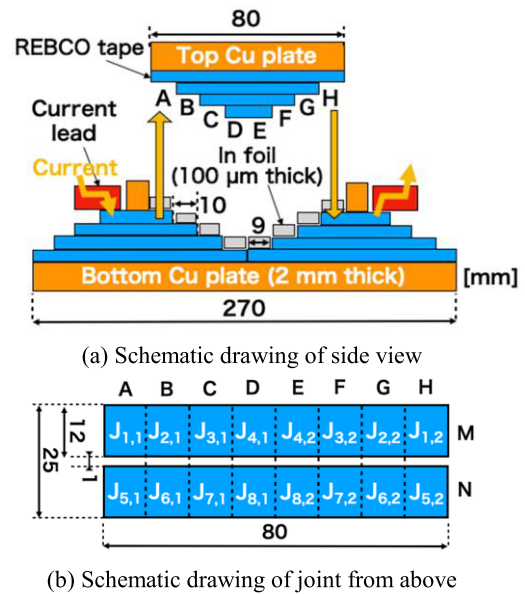


Fig. 1 Design of two-row-four-layer joint sample.

joint surface was 9 mm. The joint section was sandwiched between 2-mm thick copper that formed a copper jacket. The gap between the rows was 1 mm.

The surface of the copper stabilizer of each REBCO tape, which correspond to the joint surface, was ground using sandpaper with abrasive particles having a diameter of 81 μm . The surface was chemically deoxidized using a commercial flux (SUSSOL-F, Hakko corp., Osaka, Japan) that contains ZnCl (35 - 45%) and NH_3Cl (< 10%), and the surface was cleaned using ethanol. Similarly, the surface of the indium used as bonding material was also cleaned using ethanol.

Figure 2 illustrates the two fabrication procedures. In the “simple-stack procedure,” the REBCO tapes and indium foil were prepared and stacked over the bottom copper plate in a layered manner. The top copper plate was put over the stacks; thereafter, the sample was ready for pressing. In the “joint-piece procedure,” the REBCO tapes were bonded on the top and bottom copper plate to form an integrated joint piece and conductor region, as shown in Fig. 2 (b). Indium foils with 50- μm thicknesses were inserted between the REBCO tapes. A pressure of 40 MPa accompanied by heat treatment at 170°C was applied to melt the indium and bond the tapes. The thicknesses between the contact surface and the copper plate in the joint piece part (joint piece thickness) and the conductor region (conductor thickness) at each lap joint were measured at six random points using a micrometer (MDC-25SB, Mitutoyo Corporation, Kanagawa, Japan) prior to joining. The indium foils for each lap joint were placed over each contact surface at the conductor region. Subsequently, the integrated joint piece was placed over the conductor region.

Figure 3 shows the sum of the averaged thickness of the integrated joint piece and the conductor region (to-

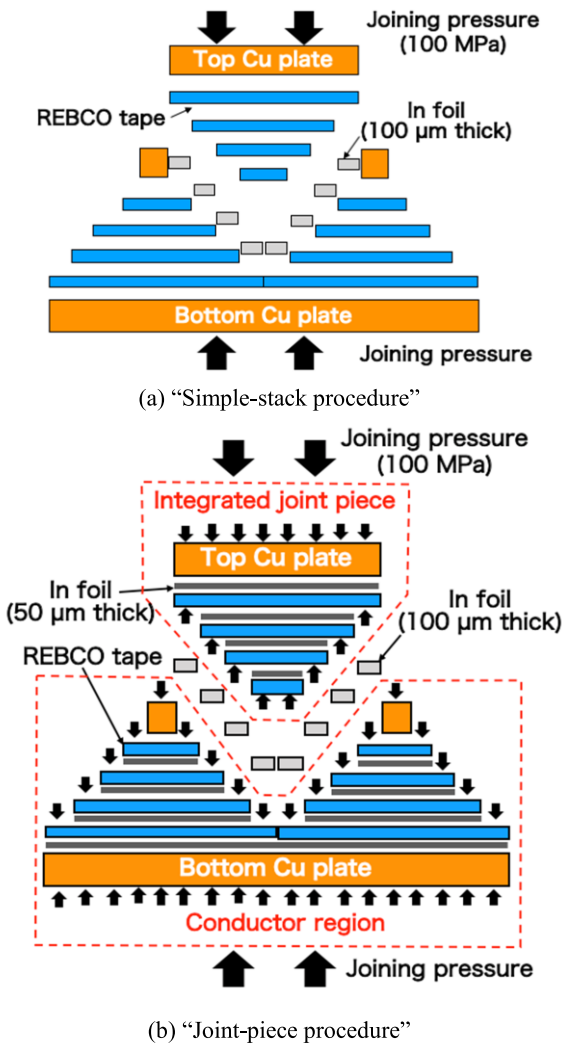
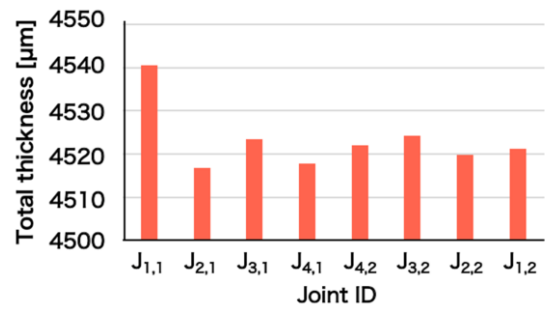


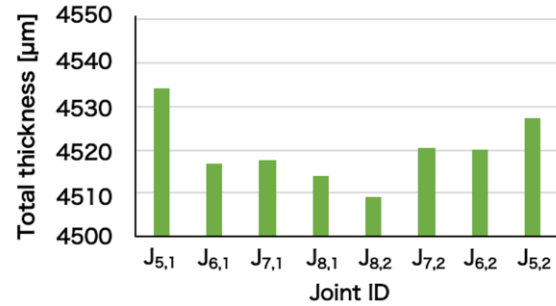
Fig. 2 Fabrication of procedures of bridge-type mechanical lap joint of two-row-four-layer STARS conductors.

tal thickness), and Fig. 4 presents the difference between the maximum and minimum values of the six thicknesses (thickness range) measured at each lap joint for the sample obtained via the “joint-piece procedure.” The variation in the total thicknesses is less than 30 μm, which is lesser than the thickness of the indium foil. Although the joining pressure could be uniformized by the inserted indium foil, it is possible that this difference induces inhomogeneity in the pressure distribution during joining, thereby resulting in high contact resistivity. The range of the variation in the thickness, which indicates the flatness of the contact surface, is another factor that may affect the stress during joining and consequently increase contact resistivity. These characteristics should be considered when discussing the evaluated contact resistivity.

During the process of joining, each joint sample was sandwiched by two flat stainless bars and pressed under a joining pressure of 100 MPa, using bolts [5]. The samples were heated at 120°C for 30 min in an electric furnace. Subsequently, a pressure of 100 MPa was applied

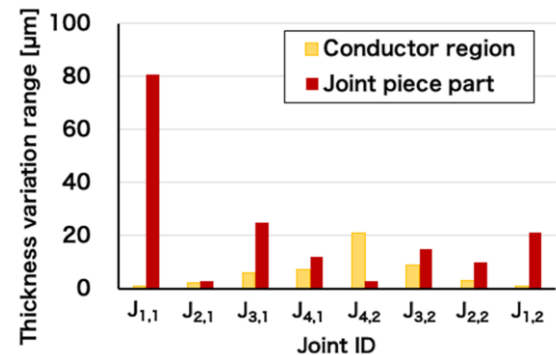


(a) Individual layer number $i = 1 - 4$

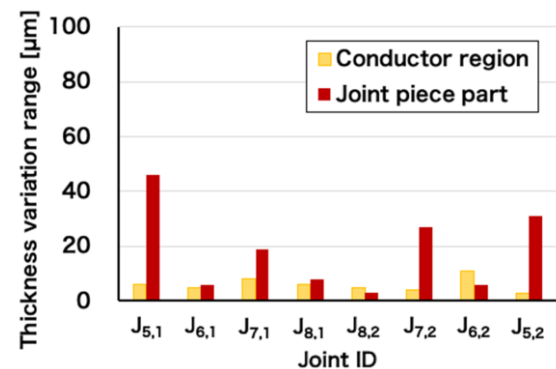


(b) Individual layer number $i = 5 - 8$

Fig. 3 Total thickness of the sample fabricated by the “joint-piece procedure”.



(a) Individual layer number $i = 1 - 4$



(b) Individual layer number $i = 5 - 8$

Fig. 4 Thickness variation range of the sample fabricated via the “joint-piece procedure”.

for an additional 30 min, because there was a decrease in the pressure owing to the stress relaxation induced by the heat treatment. Furthermore, a pressure of 100 MPa was reapplied when the joint sample was cooled down to room temperature that approximately 20°C.

2.2 Contact resistivity evaluation

Each joint sample was positioned as shown in Fig. 5 to observe the contact interfaces using a microfocus X-ray CT scan (TXS-300 TESCO corp., Kanagawa, Japan). The X-ray tube voltage and X-ray tube current were set to 230 kV and 180 μ A, respectively. A copper filter with a thickness of 0.5 mm was employed. The number of projections was 2000, and the obtained resolution was 20.9 μ m/pixel. As each lap joint has two contact interfaces, k is used to distinguish the contact interfaces. The contact areas, $S_{XCT i,j,k}$, were extracted and calculated using a technique introduced in the previous study [16].

During the evaluation of joint resistance, each sample was cooled using liquid nitrogen (77 K), and the joint resistance of each layer (i.e., sum of two single lap joints), $R_{\text{joint } i}$, was calculated using a system of equations involving the measured voltage and total applied current. In the measurement, currents up to 100 A were separately applied to each layer. As shown in Fig. 1, the current leads are set as $J_{1,1}$ and $J_{1,2}$, or $J_{5,1}$ and $J_{5,2}$ as an example. Ten sets of attachable potential probes were employed to simultaneously measure the voltage drop across each layer, top copper plate, and bottom copper plate, for monitoring the current sharing. Current was applied to each layer twice to confirm the reproducibility of the measurements. In the case where the layer l was energized, the measured voltage of the individual layer i ($V_{i,l}$), voltages of the top and bottom copper plates (i.e., $V_{\text{Cu Top } l}$ and $V_{\text{Cu Bottom } l}$, respectively) and total applied current ($I_{\text{total } l}$) can be expressed as

$$V_{i,l} = R_i \times I_{i,l}, \quad (1)$$

$$V_{\text{Cu Top } l} = R_{\text{Cu Top}} \times I_{\text{Cu Top } l}, \quad (2)$$

$$V_{\text{Cu Bottom } l} = R_{\text{Cu Bottom}} \times I_{\text{Cu Bottom } l}, \quad (3)$$

$$I_{\text{total } l} = \sum_{i=1}^8 (I_{i,l}) + I_{\text{Cu Top } l} + I_{\text{Cu Bottom } l}, \quad (4)$$

where the $I_{i,l}$, $I_{\text{Cu Top } l}$, and $I_{\text{Cu Bottom } l}$ are the currents of the layer number i , top copper plate, and bottom copper plate, respectively. The values of $R_{\text{Cu Top}}$ and $R_{\text{Cu Bottom}}$ were known. The resistance of each layer R_i corresponds to the joint resistance of each numbered layer. R_i was calculated based on the current-voltage slope (I - V curve) by applying the least-squares approach.

The thickness of each lap joint was measured to calculate the thickness of the resulting indium, $d_{\text{In } i,j}$, for evaluating contact resistivity. The sample fabricated using the “simple-stack procedure” was carefully disassembled to individual layers, and the thickness of each lap joint was measured. The resulting thickness of indium is calculated

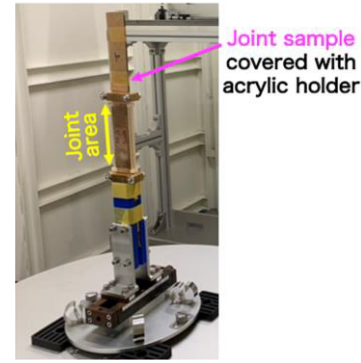


Fig. 5 Sample set up for X-ray CT scan.

by subtracting the thicknesses of two REBCO tapes from the thickness of the joint section. For the “joint-piece procedure,” the thickness between two copper plates was measured, because each lap joint could not be accessed. The resulting thickness of indium was obtained by subtracting the thicknesses of the copper plates and five REBCO tapes from the distance between two copper plates.

The contact resistances can be calculated after acquiring the contact area $S_{XCT i,j,k}$, joint resistance $R_{\text{joint } i}$, and resulting indium thickness, $d_{\text{In } i,j}$. $R_{\text{joint } i}$ is the sum of the resistances of the silver layer, copper layer of the REBCO tape, resistance of the resulting indium foil, interlayer resistance inside the REBCO tapes, and contact resistances. The sum of four contact resistances of the layer number i , $\sum_{j=1}^2 \sum_{k=1}^2 R_{\text{contact } i,j,k}$, can be expressed as

$$\begin{aligned} & \sum_{j=1}^2 \sum_{k=1}^2 R_{\text{contact } i,j,k} \\ &= R_{\text{joint } i} - \sum_{j=1}^2 \left(\begin{array}{c} \sum_{k=1}^2 \left(\frac{\rho_{\text{Ag},77\text{K}} \frac{d_{\text{Ag}}}{S_{XCT i,j,k}}}{1} \right) \\ + \rho_{\text{inter},77\text{K}} \frac{d_{\text{Cu}}}{S_{XCT i,j,k}} \\ + \rho_{\text{Cu},77\text{K}} \frac{d_{\text{Cu}}}{S_{XCT i,j,k}} \\ + \rho_{\text{In},77\text{K}} \frac{d_{\text{In } i,j}}{\sqrt{S_{XCT i,j,1}} \sqrt{S_{XCT i,j,2}}} \end{array} \right), \end{aligned} \quad (5)$$

where $\rho_{\text{Ag},77\text{K}}$, $\rho_{\text{Cu},77\text{K}}$, and $\rho_{\text{In},77\text{K}}$, are the resistivities of silver, copper, and indium at 77 K, respectively ($\rho_{\text{Ag},77\text{K}} = 2.70 \times 10^{-9} \Omega\text{m}$, $\rho_{\text{Cu},77\text{K}} = 2.10 \times 10^{-9} \Omega\text{m}$, and $\rho_{\text{In},77\text{K}} = 1.67 \times 10^{-8} \Omega\text{m}$ [19]); d_{Ag} and d_{Cu} are the thicknesses of silver layer and copper layer of the REBCO tape, respectively. $\rho_{\text{inter},77\text{K}}$ ($= 4.4 \text{ p}\Omega\text{m}^2$) is the interlayer resistivity measured via the contact-probing CTL method.

As the contact resistance of each contact interface could not be evaluated separately, the average contact resistivity of each layer was utilized in the analysis. The contact resistivity of layer i , $\rho_{\text{contact } i}$, can be expressed as

follows:

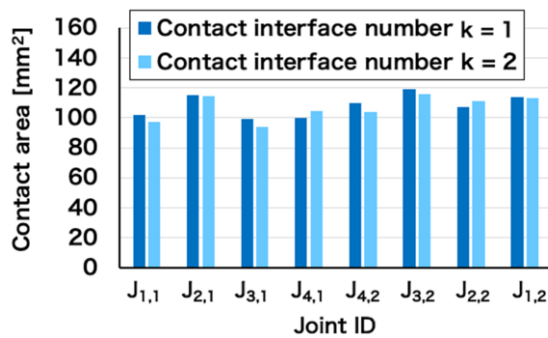
$$\rho_{\text{contact } i} = \sum_{j=1}^2 \sum_{k=1}^2 R_{\text{contact } i,j,k} \times \frac{1}{\sum_{j=1}^2 \sum_{k=1}^2 \left(\frac{1}{S_{\text{XCT } i,j,k}} \right)}. \tag{6}$$

3. Result and Discussion

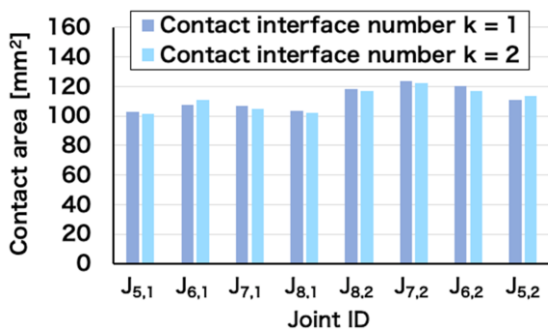
The contact area obtained when using the “simple-stack procedure” and the “joint-piece procedure” at each lap joint are depicted in Fig. 6 and Fig. 7, respectively. The contact area of the joint sample fabricated via the “joint-piece procedure” tends to be smaller than that of the sample fabricated via the “simple-stack procedure” as well as the ideal contact area of 120 mm². This result was considered from the perspective of the joint length. According to the joint sample design shown in Fig. 1, the joint length for each joint is 10 mm. If the REBCO tapes are misaligned during the layering process, the actual joint length is expected to be longer or shorter than this designed joint length: consequently, an increment or a decrement in the contact area is also expected. Therefore, the correlation between the contact area and the actual joint length was evaluated. The lengths at the center of the joint along the longitudinal direction were evaluated using the contact interface images as a representative of the actual joint lengths and compared with the contact area, as shown in Fig. 8. The correlation coefficient for the sample obtained using the “simple-stack procedure” was 0.72, and that for the sam-

ple obtained using the “joint-piece procedure” was 0.98. A comparison between the actual joint lengths and the contact area indicated a strong correlation between these two parameters. Therefore, misalignment of the REBCO tape results in small contact areas; this can be avoided by careful positioning during the fabricating process. However, considering that contact resistivity indicates the contact condition of the contact interface, this difference in the contact area does not affect the contact resistivity.

As the contact resistivity is an average value of one layer involving two lap joints, we focused on the features representing one layer. As each layer has two lap joints and each lap joint has two contact interfaces, the sum of the four contact areas was considered. Figure 9 presents a comparison between the contact resistivity and the sum of four contact areas at each layer. The contact resistivities obtained when using the “simple-stack procedure” ranges from 2.41 - 5.15 pΩm², which is similar to those obtained when using the “joint-piece procedure,” which are in the range of 1.98 - 6.07 pΩm². Prior to this empirical evaluation, the “simple-stack procedure” was considered to have higher contact resistivity than the “joint-piece procedure” and to be related to the “dog-bone” configuration of an electroplated type REBCO tape. The edge-thick configuration in the micrometer order would result in an uneven contact surface, thereby creating non-uniform joint pressure. This unevenness would accumulate during the stack-

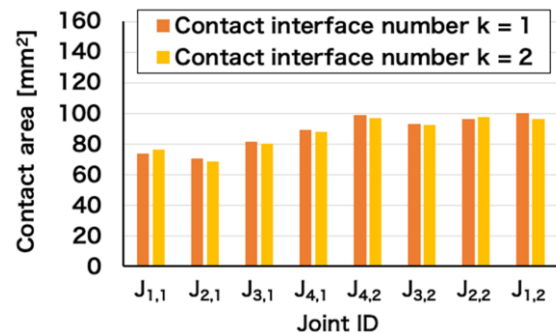


(a) Individual layer number *i* = 1 - 4

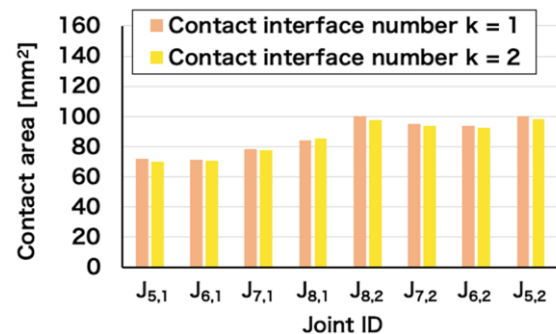


(b) Individual layer number *i* = 5 - 8

Fig. 6 Contact area of sample fabricated via the “simple-stack procedure”.

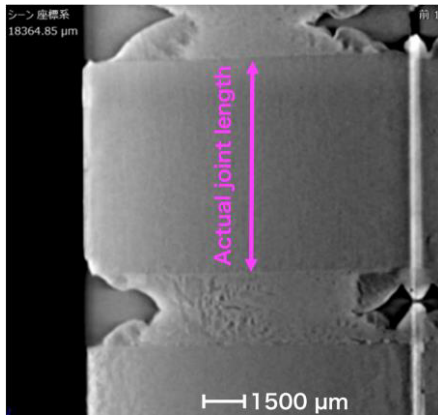


(a) Individual layer number *i* = 1 - 4

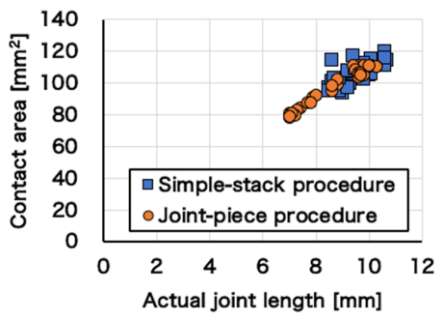


(b) Individual layer number *i* = 5 - 8

Fig. 7 Contact area of sample fabricated via the “joint-piece procedure”.



(a) Location of actual joint length



(b) Correlation between contact area and actual joint length

Fig. 8 Evaluation for actual joint length of the joint.

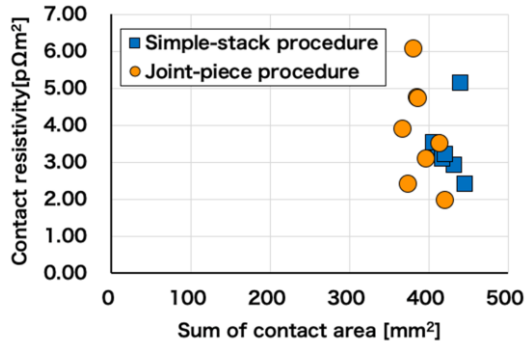
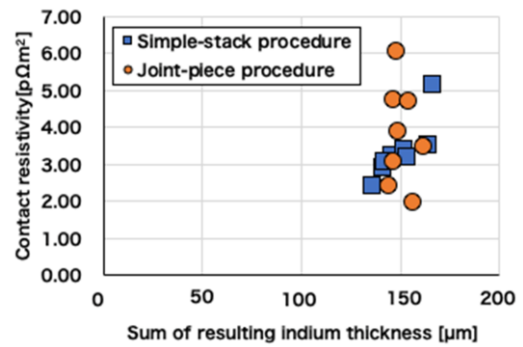


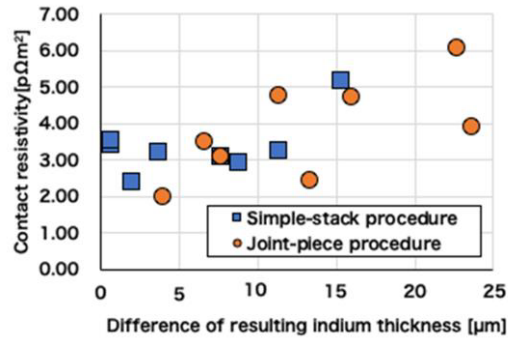
Fig. 9 Comparison of contact resistivity with contact area.

ing process of the “simple-stack procedure;” however, it would be absorbed by the indium used to fix the layers in the “joint-piece procedure.” Although the contact resistivities obtained in the “simple-stack procedure” were expected to be higher than those obtained using the “joint-piece procedure” because of the aforementioned feature of the REBCO tapes, this tendency could not be confirmed. A comparison reveals that there is no correlation between the contact resistivity and the contact area. Particularly high contact resistivity is observed at each joint sample. The reason for these high contact resistivities layer needs to be unveiled for improving the contact condition.

Considering that the joining pressure is one of the most important factors affecting contact resistance, which



(a) Correlation with sum of resulting indium thickness



(b) Correlation with difference of resulting indium thickness

Fig. 10 Correlation between contact resistivity and resulting indium thickness.

induces plastic deformation of the indium foil, the contact resistivity was compared with the resulting indium thickness, as depicted in Fig. 10. We firstly focused on the results of the “simple-stack procedure.” The relatively higher resulting indium thickness can be considered to reflect the low joining pressure. Therefore, it would be beneficial to compare the sum of the two resulting indium thicknesses of each layer and the contact resistivity, as shown in Fig. 10(a). However, this result does not completely explain the high contact resistivity, because another layer with a similar resulting indium thicknesses exhibits lower contact resistivity. The differences between the two resulting indium thicknesses of each layer, which are considered to be related to the imbalance of the joining pressure, were also compared. The high contact resistivity corresponds to the greatest difference in the resulting indium thickness in Fig. 10(b). Therefore, the non-uniform joining pressure is considered to be the reason for increasing contact resistivity during joining when using the “simple-stack procedure;” contrarily, the sample fabricated via exhibits a different tendency in both these comparisons, as shown in Fig. 10. This observation is partially attributed to the uncertainty arising from the resulting indium thickness evaluation due to the inaccessibility of each joint. An additional consideration can be established using the premise that the contact resistivity is the average value of two lap joints. The imbalance of joint pressure causes the pressure

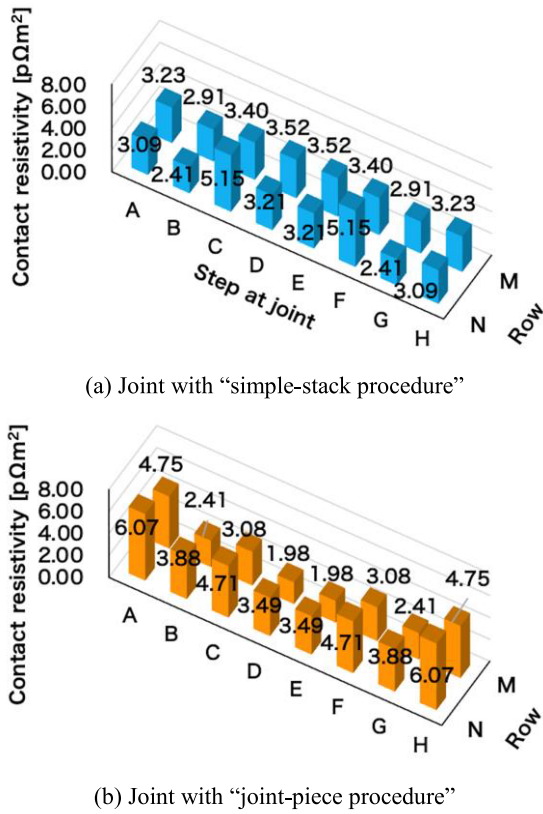


Fig. 11 Contact resistivity of each numbered layer.

to be concentrated on one lap joint, thereby decreasing the contact resistivity of the same lap joint and subsequently reducing the average of the two lap joints. Aside from the correlation in the "simple-stack procedure," the imbalanced joint pressure can be considered as the cause for the variation in contact resistivity. The difference in the resulting indium thicknesses lower than $10\ \mu\text{m}$ can be deemed as a threshold of uniform pressurization and a contact resistivity of $4\ \text{p}\Omega\text{m}^2$. However, this tendency still does not completely explain the high contact resistivity in the joint sample obtained via the "joint-piece procedure." Therefore, another comprehensive approach was considered.

The contact resistivity of each numbered layer is arrayed according to the location of the joint, as shown in Fig. 11. Based on the contact resistivities shown in Fig. 11 (a), we identified the joints located at steps C and F in row N and determine that they exhibited the highest contact resistivity, in the case of the "simple-stack procedure." In the case of the "joint-piece procedure," the lowest contact resistivity was observed at the center, i.e., at steps D and E in row M. On the contrary, the highest contact resistivity was observed at the side, i.e., at steps A and H in row N. The contact resistivity gradually increased from the center of row M to the side of row N. We first considered the correlation with the total thickness measured prior to joining. As shown in Fig. 3, $J_{1,1}$ and $J_{1,2}$, which correspond to steps A and H in row M, exhibited the highest variation. However, as the contact resistivity of these steps

were not the highest, the correlation could not be identified. Subsequently, the thickness variation range shown in Fig. 4 was considered. $J_{1,1}$ and $J_{5,1}$, which were located at step A in row M and row N, respectively, exhibited a relatively larger thickness variation range, as compared to the other joints. This indicated that the contact surface at these joints was uneven. However, the contact resistivity at step A in row M was less than that at step A in row N, which contradicts the result that $J_{1,1}$ has a more uneven contact surface. This uneven surface could not completely explain the highest contact resistivity observed at step A in row N. Finally, the situation of pressurizing was considered. Although the indium foil was plastically deformed due to the joining pressure with heat treatment, a low stress would decrease the real contact area at the contact interface and increase contact resistance, according to the theory of electric contacts [20]. Considering that the pressure was applied manually by fastening the bolts in turns, an inhomogeneous joining pressure would occasionally occur. If the joining pressure is concentrated on the center of row M, the pressure at the side of row N would be low. This reasonably explains the location distribution of the contact resistivities obtained when using the "joint-piece procedure." Therefore, an inhomogeneous joining pressure is considered to be the primary factor that causes a high contact resistivity in the "joint-piece procedure."

Using the acquired contact resistivity, the effect of high contact resistivity was evaluated by extrapolating the joint resistance at the operating conditions of the helical coil in FFHR [2, 7]. The STARS conductor consists of twenty layers and two rows of 15-mm-wide copper-stabilized REBCO tapes, for carrying 94 kA of current. The length of each joint is estimated to be 25 mm (i.e., the total length of one bridge joint is 1 m), and a joint area, S_{joint} of $375\ \text{mm}^2$ is calculated by multiplying the joint length and the width of the REBCO tape. The operating temperature is 20 K. The joint resistance can be expressed as follows:

$$\begin{aligned}
 R_{\text{joint}} = & 2\rho_{\text{Cu},20\text{K}} \frac{d_{\text{Cu}}}{S_{\text{joint}}} + 2\rho_{\text{Ag},20\text{K}} \frac{d_{\text{Ag}}}{S_{\text{joint}}} \\
 & + 2\rho_{\text{inter},20\text{K}} \frac{1}{S_{\text{joint}}} + 2\rho_{\text{contact},20\text{K}} \frac{1}{S_{\text{joint}}} \\
 & + \rho_{\text{in},20\text{K}} \frac{d_{\text{In}}}{S_{\text{joint}}}, \quad (7)
 \end{aligned}$$

where $\rho_{\text{Ag},20\text{K}}$, $\rho_{\text{Cu},20\text{K}}$, and $\rho_{\text{In},20\text{K}}$, are the resistivities of silver, copper, and indium, respectively, at 20 K ($\rho_{\text{Ag},20\text{K}} = 0.3 \times 10^{-10}\ \Omega\text{m}$, $\rho_{\text{Cu},20\text{K}} = 1.7 \times 10^{-10}\ \Omega\text{m}$, $\rho_{\text{In},20\text{K}} = 1.6 \times 10^{-9}\ \Omega\text{m}$ [19]); d_{Ag} , and d_{Cu} , are the thicknesses of silver layer and copper layer of the REBCO tape, respectively. d_{In} denotes the thickness of indium foil, which was assumed to be $100\ \mu\text{m}$. $\rho_{\text{inter},20\text{K}}$ ($= 4.4\ \text{p}\Omega\text{m}^2$) is the interlayer resistivity utilized in this study and the temperature dependency has been reported in a previous study [18]. $\rho_{\text{contact},20\text{K}}$ is the contact resistivity at the contact interface and the temperature dependency evaluated in a previous

study [21] was introduced to extrapolate the value at 20 K.

According to a previous study [7], in the case of the half-pitch conductor segments, a joint resistance of 5 n Ω or each joint section is comparable to the helical coil option using low-temperature superconductor in terms of the electric power required to run a cryo-plant. As the layers are connected in parallel in a conductor, one joint at each layer required to be less than the joint resistance of 200 n Ω . Substituting the highest contact resistivity of 6.07 p Ωm^2 in the ρ_{contact} of Eq. (7), the joint resistant of one joint is estimated to be 39 n Ω . These values are acceptable for the joint resistance of 200 n Ω . Besides, the ρ_{inter} of the REBCO tape used in this study was relatively higher than the value reported in a previous study [18]. A lower joint resistance can be achieved by utilizing a REBCO tape with lower interlayer resistance, because the interlayer resistance depends on the process of manufacturing the REBCO tape and can be predicted using the contact-probing CTL method.

4. Conclusion

In this study, we fabricated joint samples using the “simple-stack procedure” and the “joint-piece procedure” to compare the differences in the contact conditions resulting from the joining procedure. The average contact resistivity of each layer was evaluated based on the results of joint thickness, joint resistance, and contact area, which were observed using an X-ray CT scan. The contact areas of the sample fabricated via the “joint-piece procedure” were confirmed to be reduced owing to a misalignment of the REBCO tapes; however, this result is avoidable and did not affect contact resistivity. The contact resistivities of the sample fabricated using the “simple-stack procedure” ranged from 2.41 - 5.15 p Ωm^2 , whereas those of the sample fabricated via the “joint-piece procedure” ranged from 1.98 - 6.07 p Ωm^2 . Moreover, there were no trends in contact resistivity with respect to the joining procedures. Inhomogeneous joining pressure is a critical factor that results in variations in the contact resistivity for both the fabrication procedures. The highest contact resistivity achieved in this study is acceptable in terms of the electric power required for a cryo-plant.

The electrical performances of the joints fabricated using the two procedures were similar on the two-row-four-layer conductor scale. Considering the larger conductors used in fusion reactors, it is necessary to resolve the mis-

alignments in individual REBCO tape joints in the case of the “simple-stack procedure,” as confirmed in previous studies [12, 22]. In the “joint-piece procedure,” the risk of misalignment is considered to comparatively lesser, whereas future studies should focus on the manufacturability of large-scale integrated joint pieces.

Acknowledgments

This work was supported in part by Grants-in-Aid for JSPS research Fellow grant no. 17J02122, Grant-in-Aid for Scientific Research (S) grant no. 26220913, Grants-in-Aid for Scientific Research (B) grant no. 17H03507 and by the National Institute for Fusion Science (NIFS) Collaboration Research Program grant no. NIFS19KECF026.

- [1] N. Yanagi *et al.*, Fusion Sci. Technol. **60**, 648 (2011).
- [2] N. Yanagi *et al.*, IEEE Trans. Appl. Supercond. **24**, 4202805 (2014).
- [3] N. Yanagi *et al.*, Nucl. Fusion **55**, 053021 (2015).
- [4] A. Sagara *et al.*, Fusion Eng. Des. **89**, 2114 (2014).
- [5] A. Sagara *et al.*, Nucl. Fusion **57**, 086046 (2017).
- [6] S. Ito *et al.*, Plasma Fusion Res. **9**, 3405086 (2014).
- [7] S. Ito *et al.*, IEEE Trans. Appl. Supercond. **26**, 4201510 (2016).
- [8] T. Nishio *et al.*, IEEE Trans. Appl. Supercond. **26**, 4800505 (2016).
- [9] T. Nishio *et al.*, IEEE Trans. Appl. Supercond. **27**, 4603305 (2017).
- [10] H. Hashizume *et al.*, Nucl. Fusion **58**, 026014 (2018).
- [11] S. Ito *et al.*, Fusion Eng. Des. **136**, 239 (2018).
- [12] S. Ito *et al.*, Fusion Eng. Des. **146**, 590 (2019).
- [13] C. Scheuerlein *et al.*, Supercond. Sci. Technol. **24**, 115004 (2011).
- [14] M. Inoue *et al.*, IEEE Trans. Appl. Supercond. **26**, 6201004 (2016).
- [15] I. Tiseanu *et al.*, Fusion Eng. Des. **88**, 1613 (2013).
- [16] W. Chen *et al.*, Fusion Eng. Des. **148**, 111284 (2019).
- [17] N. Bagrets *et al.*, IEEE Trans. Appl. Supercond. **28**, 6600204 (2018).
- [18] R. Hayasaka *et al.*, IEEE Trans. Appl. Supercond. **29**, 9000805 (2019).
- [19] J.W. Ekin, *Experimental Techniques for Low-Temperature Measurements* (Oxford Univ. Press, Boulder, 2006).
- [20] R. Holm, *Electric Contacts Theory and Application* (Spring-Verlag, Berlin Heidelberg 1967).
- [21] S. Ito *et al.*, IEEE Trans. Appl. Supercond. **26**, 6601505 (2016).
- [22] S. Ito *et al.*, IEEE Trans. Appl. Supercond. **24**, 4602305 (2014).